Dynamic Positioned Semi-Submersible Platform Motion with Riser in Ultra Deep Water

Celso Kazuyuki Morooka, State University of Campinas

Marcio Yamamoto, State University of Campinas

ABSTRACT

The objective of this paper is to describe the dynamics of semi-submersible drilling platforms under environmental loads in an ultra deep water scenario. A floating platform connected to the sea bottom by a long slender pipe is taken into account. Current and wave acting on the floating platform and along the riser length are considered.

Numerical simulation in time domain has been developed using a non-linear model for the floating platform dynamics with an ultra deep drilling riser. Dynamics of a drilling riser and the dynamic positioning system (DPS) of the platform are also included in the numerical model. Simulation results in time domain for the floating platform motion with DP control and riser displacement behavior are shown. Discussions in terms of riser design and optimization of dynamic positioning system control are carried out.

Keywords: *Vessel dynamics, Dynamic Positioning System, Riser Dynamics, computational simulation.*

1. INTRODUCTION

The recent discoveries of large petroleum fields are, in general, in deep (300-1500 m of water depth) and ultra deep water (1500-3000 m w.d.). For operations of Exploration & Production (E&P) in these depths, it is necessary the use of floating platform such as ship hull platforms (Drillships) and semi-submersibles platforms.

To accomplish the E&P operations, a floating platform must be kept stationary on a desired location. In the most common case, a platform uses a mooring system to keep stationary, but for deep and ultra deep water the mooring system becomes uneconomical and/or unpractical. Then Dynamic Positioning System (DPS) overcomes this problem: a feedback control system receives the platform position data from sensor system, and then controls the thrusters installed on the bottom of the platform hull.

In addition, for offshore petroleum E&P operations, the well is connected to the platform deck through a slender pipe that is called riser by the petroleum industry.

In a drilling scenario, only one rigid vertical riser connects the wellhead to rig floor at platform deck. A drill string reaches the bottom well through the riser. Furthermore, the drilling mud is injected through drill string, and return to rig floor carrying drilling cuts though annular between the riser and drill string.

The numerical simulator developed for this paper had one degree of freedom (sway) for the platform dynamics (Yamamoto & Morooka, 2005), and a quasi 3-D approach for riser dynamics (Ferrari Jr. & Bearman, 1999, Morooka et al., 2003, Morooka et al., 2005).

2. DYNAMIC POSITIONING SYSTEM

According to Morgan (1978), a DPS can be divided basically into 4 sub-systems (Figure 1):

- Sensor system;
- Controller;
- Thruster system; and
- Power system.

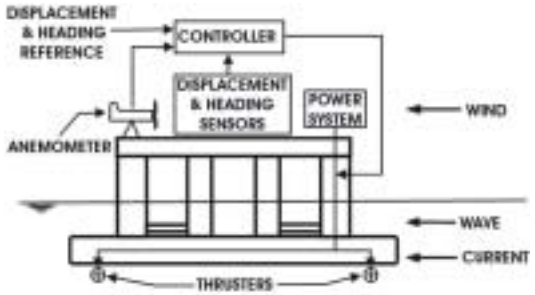

Figure 1. An example of DPS.

The sensor system is responsible for the measurement of platform displacement and environmental parameters. The platform displacement is measured by both Differential Global Positioning System (DGPS) and the Acoustic Position Reference System. The most common heading sensor is the gyrocompass due to its robustness and its proven application in marine systems (Morgan, 1978). Usually, wind is the only environmental parameter that is measured. Wind speed and direction are measured by an anemometer and the data are used for wind feed-forward control.

The second element of a DPS is the controller. It receives data about displacement, heading and environmental parameters from the sensor system, and the displacement and heading reference from DPS operator, then it computes the force and momentum required to counterbalance the environmental loads and to mitigate the error signal (difference between the real position and reference position). Further it controls thrusters action. See the block diagram of DPS in Figure 2.

The third element of a DPS is the thrusters system. Its function is to generate the forces and moments that will counteract the environmental loads and thus keep the platform within the tolerance radius.

Finally, the fourth element of a DPS is the electrical power generating system. Its choice depends mainly on the number of thrusters and on whether the thrusters are driven by AC or DC motors.

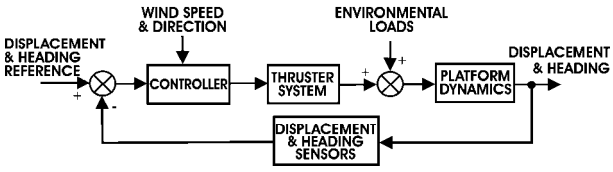

Figure 2. A block diagram of DPS.

3. MATHEMATICS

3.1 Equation of Motion for a Floating Platform

Floating platform dynamics can be modelled as a nonlinear mass-spring-damper system. In this work, the simulation program was coded using the integral-differential equation proposed by Cummins (1962), as shown in Eq.(1).

$$(M+m)\cdot\ddot{x}+\int_{-\infty}^{\infty}K(t-\tau)\cdot\dot{x}(\tau)\cdot d\tau+ +B\cdot|\dot{x}|\cdot\dot{x}+C\cdot x=F_T \quad (1)$$

In the above equation, x is the platform position and the dot above means the time derivative; M is the platform mass; m is a constant added mass is calculated by Equation (2); K is an impulse response function defined by Equation (3); B is the viscous damping coefficient; and F_T is the sum of external forces (environmental load, riser reaction and thrust) that acts on the platform.

$$m=a(\omega)+\frac{1}{\omega}\cdot\mathrm{Im}\left[\int_{-\infty}^{\infty}K(\tau)\cdot\exp(i\cdot\omega\cdot t)\cdot dt\right] \quad (2)$$

$$K(t) = \frac{1}{2 \cdot \pi} \cdot \int b(\omega) \cdot \exp(-i \cdot \omega \cdot t) \cdot d\omega \qquad (3)$$

In the Equation (2), the variable, a, is the added mass that depends on the frequency of the system; in the Eq.(3), the variable, b, is the damping coefficient that depends on the frequency of the system; i is the imaginary unit; the operator Im(.) means the imaginary part, K is the impulse response function; t is time; and ω is the frequency.

3.2 Environmental Loads

The loads due to current that act on the platform are modelled as drag force, Equation (4).

$$F_D = \frac{1}{2} \cdot \rho \cdot C_D \cdot A \cdot |V - \dot{x}| \cdot (V - \dot{x}) \qquad (4)$$

Where A is the exposed frontal area; C_D is the drag coefficient; F_D is the drag force due current or wind; V is the velocity of fluid particle; and $\dot{x}$ is the platform velocity.

In this paper, a simplification was assumed: the interaction of wakes and vortices with columns and pontoons of the platform are neglected. Furthermore, the platform was meshed into elementary shapes in order to evaluate the overall platform drag coefficient (DnV, 1977).

The wave load can be modelled as the first two terms of Volterra series. In this paper, a simplification of these two terms, proposed by Newman (1974), is used, as shown in Equation (5).

$$F_1(t) = \sum_{j=1}^{N} \zeta_j \cdot |H_1(\omega_j)| \cdot \varepsilon_1(t, \omega_j) \qquad (5.a)$$

$$F_2(t) = 2 \cdot \left[\sum_{j=1}^{N} \zeta_j \cdot \sqrt{H_2(\omega_j, \omega_j)} \cdot \varepsilon_2(t, \omega_j) \right]^2 \qquad (5.b)$$

In the above equations, F_1 is the first-order drift force (linear), and F_2 is the second-order drift force (non-linear); ζ_j and ω_j are the elevation and frequency of j–th wave, respectively; H_1 is the first order transfer function of amplitude and H_2 is the second order transfer function of amplitude; ε_1 and ε_2 are given by Equation (6).

$$\varepsilon_1(t, \omega) = \sin(\omega \cdot t + \phi_1(\omega)) \qquad (6.a)$$

$$\varepsilon_2(t, \omega) = \cos(\omega \cdot t + \phi_2(\omega, \omega)) \qquad (6.b)$$

In the above equations, ϕ_1 & ϕ_2 are the phase transfer function of first order and second order, respectively.

3.3 Thrusters

Thruster forces can be expressed as a first-order system, as Eq.(7) shows in Time Domain (Zunderdorp and van der Vlies, 1972).

$$E_c(t) = E(t) + \tau \cdot \frac{dE}{dt} \qquad (7)$$

Where E is the force developed by the thrusters; and E_c is the force that is applied by the controller.

In this work, a time constant of 5.0 s was adopted. In order to prevent mechanical fatigue of the thruster system, the controller is not allowed to vary the value of the force continuously, but only at intervals of 20 s. The reduction of thruster force by current influx is not taken into account in the simulator.

3.4 Riser Dynamics

A riser can be modelled as a long beam with transversal loads due effects of hydrostatic and hydrodynamics pressure (Patel & Witz, 1991, Ferrari Jr. & Bearman, 1999, Morooka, et al., 2003).

Figure 3 shows the static equilibrium of an infinitesimal element of riser. Equation (8) describes the deflection of riser.

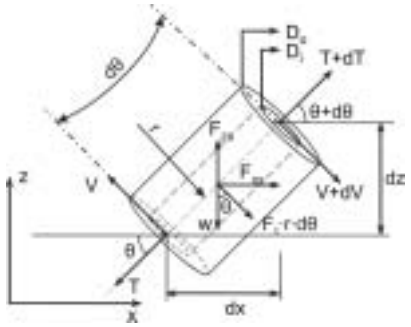

Figure 3. Infinitesimal element of riser.

$$\frac{d^2}{dz^2}\left(EI\cdot\frac{d^2x_R}{dz^2}\right)-\left(T+A_0\cdot P_0-A_I\cdot P_I\right)\cdot\frac{d^2x_R}{dz^2}$$

$$-\left[\gamma_S\cdot\left(A_0-A_I\right)-F_{ZS}-A_0\cdot\gamma_0+A_I\cdot\gamma_I\right]\cdot\frac{dx_R}{dz} \quad (8)$$
$$+m\cdot\ddot{x}_R=F_{XS}$$

In the above equation, EI means the bending stiffness; T is the axial tension of riser; A_0 and A_I are the external and internal cross sectional area of riser pipe, respectively; P_0 and P_I are the external and internal pressure that acts on the riser; γ_S, γ_0 and γ_I are the specific weights of the riser material, the external fluid and internal fluid; m is the riser mass; z is the riser length; $\ddot{x}_R$ is the riser acceleration; and F_{xs} is load in the x direction.

Then it is necessary to establish a directional convention for loads and displacements of the riser: the direction of flow is called In-Line and the transverse direction is called Transversal.

The solution of Equation (8) is obtained using the weak approach of Galerkin formulation for Finite Elements Method, and this solution is used as stiffness matrix for Equation (9) (Ferrari Jr. & Bearman, 1998; Morooka et al., 2003).

The in-line load is estimated using a modified Morison Equation (Morroka *et al.*, 2005).

The transversal load is due the shed of alternate vortices that generates a sinusoidal load in the transversal direction (Sarpkaya and Isaacson, 1981). This transversal load phenomenon is called Vibration Induced by Vortices (VIV) and special attention must be paid to this sinusoidal load because it reduces the service life of riser due the fatigue (Morooka et al., 2005). In this paper, the transversal load is described in terms of the semi-empirical methodology presented by Ferrari Jr. & Bearman (1999).

Furthermore, the structure of the riser is divided into finite elements, which the masses are concentrated in their nodes. The dynamic behavior of the riser is obtained for the in-line and transverse directions by Equation (9), reproducing a three-dimensional dynamics.

$$M\cdot\ddot{x}+B\cdot\dot{x}+K\cdot x=F \quad (9)$$

In the above equations, M is the mass matrix; B is the damping matrix and K is the stiffness matrix.

More details about riser dynamics can be found in Ferrari Jr. & Bearman (1999), Morooka et al. (2004), and Morooka et al. (2003/2005).

For the coupling between the riser and the floating platform assumes the following: the upper riser end is connected to the platform barycentre and the riser reaction on the platform is equal to riser shear force at the upper riser element, this shear force is added to term F_T of Equation (1).

4. RESULTS

In this paper, the chosen semi-submersible model (Figure 4) was the standard semi-submersible platform adopted by International Towing Tank Conference (ITTC) for comparative calculations. More details about this standard platform can be found in Vardaro (1991).

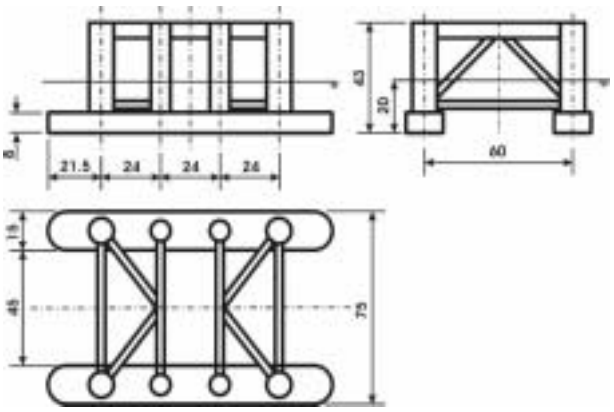

Figure 4. ITTC Platform dimensions [meters].

The riser model had the following properties:

Table1: Riser properties.

Length under water level	3000 m
Length above water level	20 m
External Diameter	0.54 m
Internal Diameter	0.4985 m
Young's Modulus	210 MPa
Material Density	7860 kg/m3
Drilling Mud Dens.	1500 kg/m3

It is assumed that platform baricenter has the local coordinate system, and the riser upper end is connected to the platform at the same point.

In addition, two PID controllers with different tuning are compared. Figure 5 features the platform displacement under a current load of 1 m/s, and Figure 6 features the platform displacement with regular wave load (height=4m, T=10s). The performance of platform DPS with and without the riser are also featured.

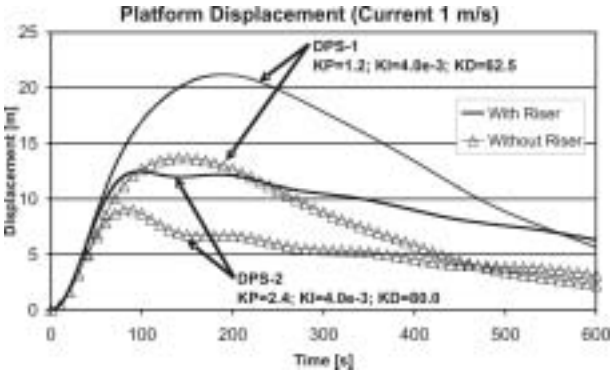

Figure 5. Performance of different controller's gains applied in the DPS (current).

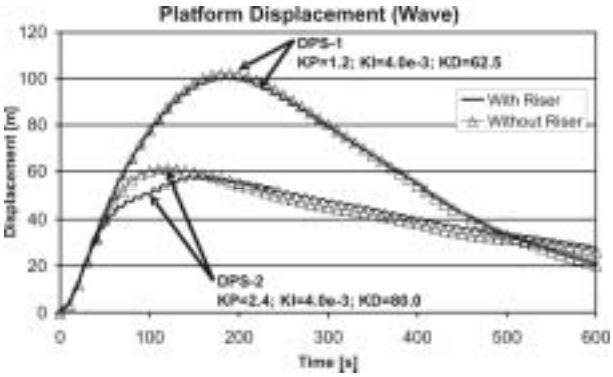

Figure 6. Performance of different controller's gains applied in the DPS (wave).

The gains set called DPS-2 has a proportional gain (K_P) higher than the set called DPS-1, and then DPS-2 converges quicker to the reference. In Figure 5, the riser presence decreases the DPS performance because the drag force on the whole riser is added to the drag force that acts on the platform. In Figure 6, the effects due the riser are lower than in the current case because the wave acts only on the riser near to the water surface.

Next, Figure 7 and Figure 8 show the riser reaction on the platform for different control gains sets and a top tension of 15,000 kN with a current of 1 m/s and a regular wave height of 4m and period of 10s, respectively.

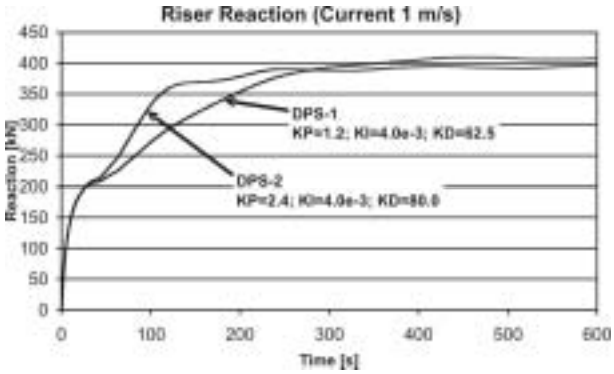

Figure 7. Riser reaction on the platform for different controller gains set (current).

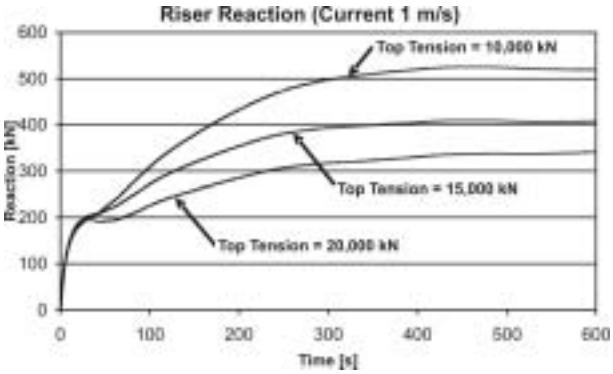

Figure 9. Riser reaction on the platform for different top tensions (current).

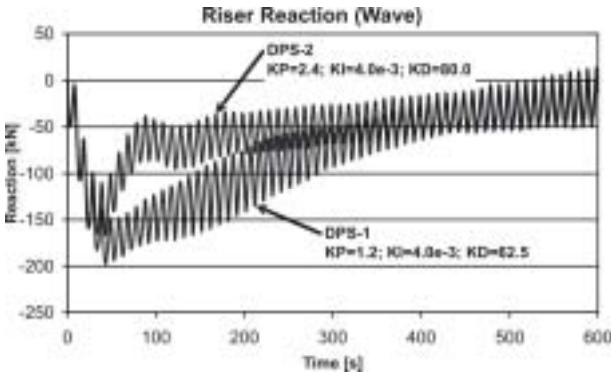

Figure 8. Riser reaction on the platform for different controller gains set (current).

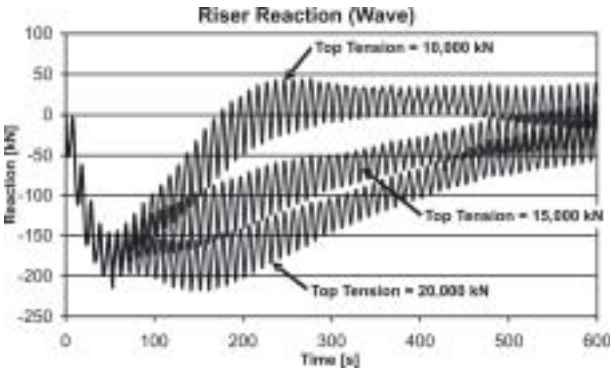

Figure 10. Riser reaction on the platform for different top tensions (wave).

In Figure 7, the riser reaction of DPS-2 reaches the maximum reaction quicker than DPS-1 because its gains set increases the systems velocity. The discontinuity around 40 s is, probably, due the system acceleration that became null around this point. The small difference between the final reactions is due the difference of terminal velocity of the two gains sets.

In Figure 8, the environmental load acts on the riser near to the surface, then the riser is displaced mainly by platform displacement, and the riser reaction is negative, DPS-2 has lower peak because it has a smaller displacement.

Following, Figures 9 and 10 show the effects of the top tension on the riser reaction on the floating platform, is assumed the gains set of DPS-1.

The increase of top tension results in the decrease of riser bending momenta and consequently the shear forces and the riser reaction on the floating platform.

Figure 11 and Figure 12 features the maximum riser displacement for different controller gain set, is assumed a top tension of 15,000 kN and a current of 1 m/s. Figure 11 shows the riser displacement in the In-Line direction where the riser displacement is due platform displacement and current load on the whole riser. Figure 12 shows the riser displacement in the Transversal direction, this displacement is due only to the Vibration Induced by Vortices (VIV).

Figures 13 & 14 feature also the maximum riser displacement for different controller gain set, but the environmental load is due regular wave with height of 4 m and period of 10 s. Figure 13 shows the riser displacement in the In-Line direction and Figure 14 for Transversal direction.

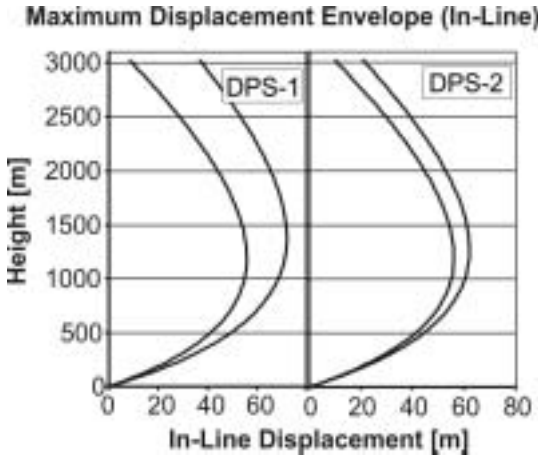

Figure 11. Maximum Riser Displacement due current for different DPS (In-Line).

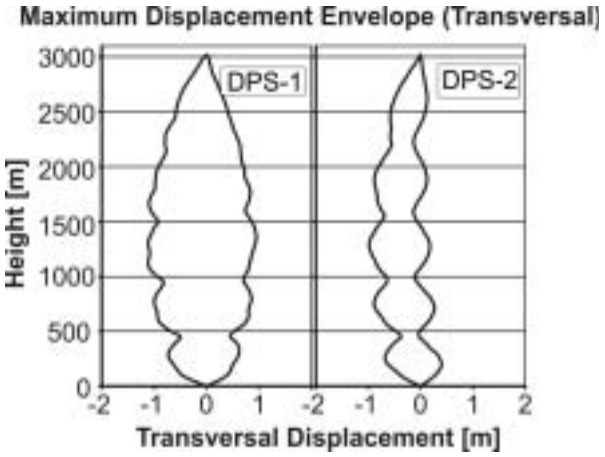

Figure 14. Maximum Riser Displacement due regular wave for different DPS (Transversal).

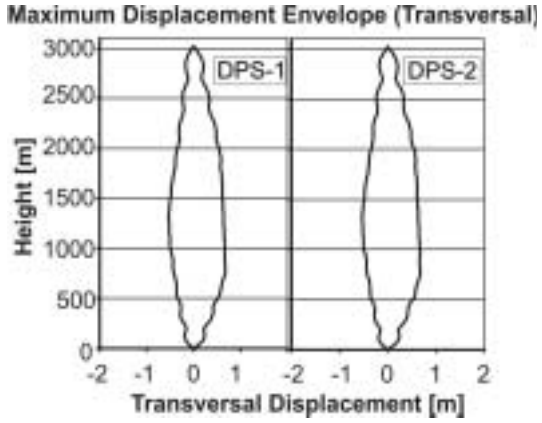

Figure 12. Maximum Riser Displacement due current for different DPS (Transversal).

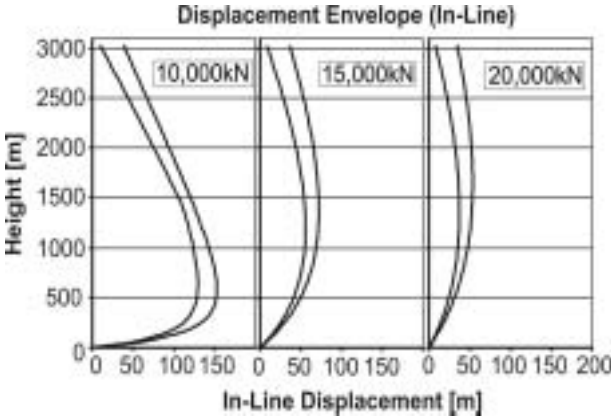

Figure 15. Maximum riser displacement due current for different top tension (In-Line).

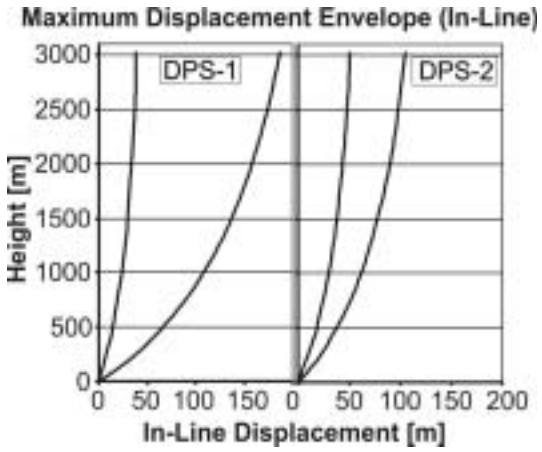

Figure 13. Maximum Riser Displacement due regular wave for different DPS (In-Line).

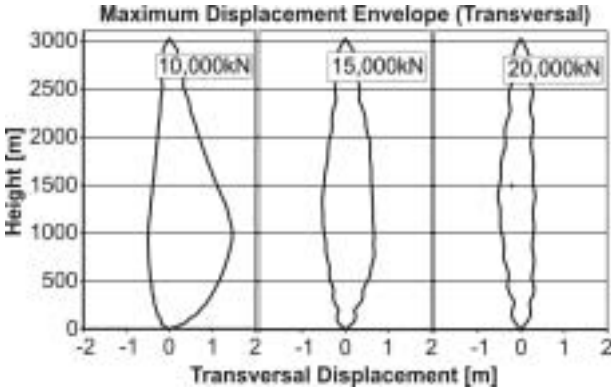

Figure 16. Maximum riser displacement due current for different top tension (Transversal).

Following, Figures 15, 16, 17 and 18 feature the effect of the top tension on the maximum displacement for current and regular wave loads.

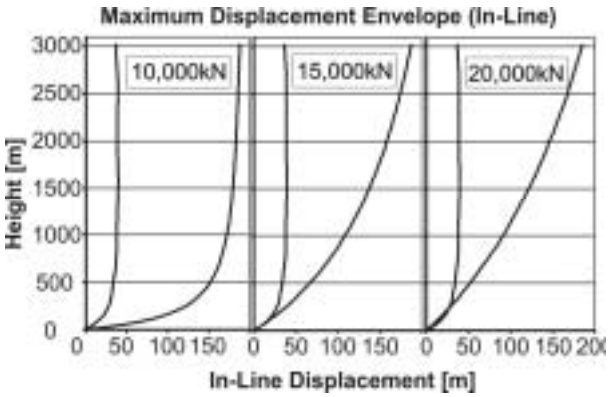

Figure 17. Maximum riser displacement due regular wave for different top tension (In-Line).

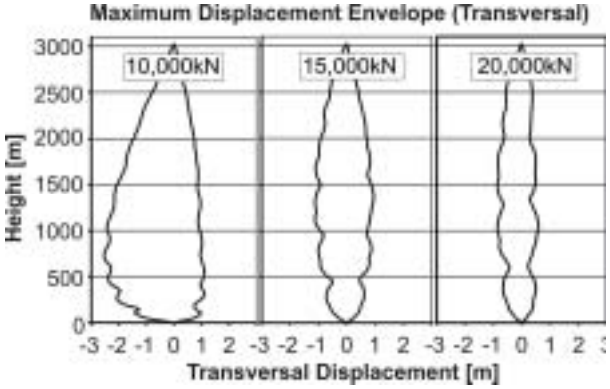

Figure 18. Maximum riser displacement due regular wave for different top tension (Transv.).

The top tension has a significant effect on the riser displacement. The top tension increase reduces the riser bending momenta and consequently the riser deflection.

5. CONCLUSION

In this paper, the dynamic behavior of a floating semi-submersible platform equipped with DPS and with drilling riser connecting the well head at sea bottom to the platform rig floor was carried out.

This paper featured the effects of the DPS controller gains over the platform displacement, riser reaction on the platform, and riser envelope of displacement. The gains affect, mainly, the platform displacement and the riser displacement in the In-Line direction.

After, the effects of top tension on the riser dynamics were featured. The top tension alters the bending moment of the riser and, consequently, the riser stiffness.

6. ACKNOWLEDGMENTS

The authors would like to acknowledge the financial support of the Brazilian Petroleum Agency (PRH15-ANP/MCT), Petrobras, CNPq and FINEP/CTPetro.

7. REFERENCES

Cummins, W.E., 1962, “The Impulse-response Function and Ship Motions”, Schiffstechnik, Vol. 47, no. 9, pp. 101-109.

DnV, 1977, “Rules for the Design Construction and Inspection of Offshore Structures”, Appendix B: Loads, Det Norske Veritas (DnV), Oslo, Norway.

Ferrari Jr., J.A., Bearman, P.W., 1999, “Hydrodynamic Loading and Response of Offshore Risers”, Proceedings of OMAE 1999, 18th International Conference on Offshore Mechanics and Arctic Engineering (OMAE 1999), Newfoundland, Canada.

Morgan, M.J., 1978, “Dynamic Positioning of Offshore Vessels”, PPC Books Division, Tulsa.

Morooka, C.K., Kubota, H.Y., Nishimoto, K., Ferrari Jr., J.A., Ribeiro, E.J.B., 2003, “Dynamic Behavior of a Vertical Production Riser by Quasi 3D Calculations”, Proceedings of OMAE 2003, 22nd International Conference on Offshore Mechanics and Arctic

Morooka, C.K., Coelho, F.M., Ribeiro E.J.B., Ferrari Jr., J.A., Franciss, R., 2005, "Dynamic Behavior of a Vertical Riser and Service Life Reduction", Proceedings of OMAE 2005, 24th International Conference on Offshore Mechanics and Arctic Engineering (OMAE 2005), Halkidiki, Greece.

Newman, J.N., 1974, "Second-order, Slowly-varying Forces on Vessels in Irregular Waves", International Symposium on the Dynamics of Marine Vehicles and Structures in Waves, ed. R. Bishop and W.G. Price, pp. 182-186, Mechanical Engineering Publications Ltd., London.

Patel, M.H., Witz, J.A., 1991, "Compliant Offshore Structures", Butterworth-Heinemann.

Sarpkaya, T., Isaacson, M., 1981, "Mechanics of Wave Forces on Offshore Structures", Van Nostrand & Reinhold Co., 1st Edition.

Vardaro, E., 1991,"A Study of Motions of a Semi-Submersible Platform through Time Domain Simulation" (In Portuguese), M.Sc. Thesis, State University of Campinas, Campinas, Brazil.

Yamamoto, M., Morooka, C. K., 2005, "Dynamic Positioning System of Semi-Submersible Platform Using Fuzzy Control", Journal of the Brazilian Society of Mechanical Sciences & Engineering, Vol. 27, no. 4, pp. 449-455, October-December 2005.

Zunderdorp, H.J., van der Vlies, J.A., 1972, "How to Optimise a Dynamic-Stationing System", Society of Petroleum Engineers (SPE), European Spring Meeting, Amsterdam, Netherlands, SPE #3757.